# Surface states and resonances on Al(110): Ultraviolet photoemission spectroscopy and *ab initio* calculations

M. J. G. Lee,[1,*] M. Gensch,[2] A. I. Shkrebtii,[3] Th. Herrmann,[4] W. Richter,[4,5] N. Esser,[2] and Ph. Hofmann[6]
[1]*Department of Physics, University of Toronto, 60 St George Street, Toronto, Ontario, Canada M5S 1A7*
[2]*ISAS, Institute for Analytical Sciences, Department Berlin, Albert-Einstein-Strasse 9, D-12489 Berlin, Germany*
[3]*Faculty of Science, University of Ontario Institute of Technology, 2000 Simcoe Street North, Oshawa, Ontario, Canada L1H 7L7*
[4]*Institut für Festkörperphysik, TU-Berlin, Hardenbergstrasse 36, D-10623 Berlin, Germany*
[5]*Dipartimento di Fisica, Università di Roma Tor Vergata, Roma, 00133, Italy*
[6]*Department of Physics and Astronomy, University of Aarhus, Dk-8000 Aarhus C, Denmark*
(Received 27 October 2004; revised manuscript received 26 April 2005; published 2 August 2005)

The electronic structure of a clean (110) surface of crystalline aluminum is investigated experimentally by measuring the angle-resolved ultraviolet photoemission spectra at high-symmetry points of the surface Brillouin zone for photon energies in the range 10–29 eV. The binding energies and dispersions of several features in the experimental spectra are determined. The experimental data are interpreted by means of an *ab initio* full-potential linear-augmented plane-wave calculation of the surface electronic structure based on density functional theory. Two of the features in the spectra are identified as being due to emission from previously unobserved surface states and surface resonances. The effects of surface relaxation on the surface electronic structure are discussed.

DOI: 10.1103/PhysRevB.72.085408 PACS number(s): 79.60.Bm, 73.20.−r, 71.20.−b

## I. INTRODUCTION

The bulk and surface electronic properties of single crystals of a wide variety of metals have been investigated by angle-resolved ultraviolet photoemission spectroscopy (ARUPS).[1] The bulk electronic properties[2,3] and the linear optical response[4] of the prototypical free-electron metal aluminum are well understood. Several ARUPS studies of the electronic structures of the low-index surfaces of aluminum have been reported.[5–7]

In the present paper we report a combined experimental and theoretical investigation of the surface electronic structure of Al(110). Hansson and Flodstrom[5] observed features of the surface electronic structure of Al(110) at $\bar{\Gamma}$ and in the vicinity of $\bar{X}$. The experimental data were interpreted on the basis of the tight-binding model,[8] which is not well suited to nearly-free-electron metals. A pseudopotential plane-wave calculation of the surface electronic structure by Heinrichsmeier *et al.*[9] based on density functional theory (DFT) in the local density approximation (LDA) predicted additional surface states and resonances, but these predictions have not so far been tested by experiment.

The present experimental investigation of Al(110) uses synchrotron sources, which make it possible to distinguish experimentally between features of the surface and bulk electronic structures. In addition to the two features of the surface electronic structure that were observed by Hansson and Flodstrom we find a surface state at $\bar{S}$ that was predicted by Heinrichsmeier *et al.*[9] and a surface resonance at $\bar{\Gamma}$ that was not predicted by previous calculations. We also report what are, to our knowledge, the first experimental measurements of the dispersion of these four features.

In recent years, substantial progress has been made in DFT with the development of improved computational techniques and improved exchange-correlation potentials. Our experimental data are interpreted on the basis of DFT calculations in which exchange and correlation are treated in the generalized gradient approximation (GGA). In view of the nearly-free-electron character of the electronic structure of aluminum, many-body corrections are neglected.

The previously published calculations of the surface electronic structure of Al(110) (Refs. 8 and 9) assumed an ideally terminated (i.e., nonrelaxed) lattice, but it is now well established by experiment that, at room temperature and below, the surface relaxation of Al(110) involves atomic displacements in the direction normal to the surface in at least the first three atomic layers.[10,11] Bulk aluminum is face-centered cubic and is therefore optically isotropic. Al(110) is of particular interest because it is the only low-index surface of aluminum that is optically anisotropic. In recent papers[12,13] it has been shown that, in the interband regime, the reflectance anisotropy spectrum (RAS) of Al(110) is dominated by optical transitions between bulk electronic states and is therefore little affected by surface relaxation. In the present paper we compare the calculated surface electronic structure in which surface relaxation is taken into account with that for an ideally terminated lattice. We find that the binding energies of features of the surface electronic structure are only weakly influenced by surface relaxation.

## II. EXPERIMENTAL METHOD

The experiments were carried out at the Technical University (TU) in Berlin and at the synchrotron radiation source ASTRID in Aarhus. The sample was a high-purity single crystal that had been cut parallel to (110) (error of orientation 0.5°) and polished (surface roughness approximately 0.03 $\mu$). The sample was cleaned in ultrahigh vacuum (UHV) by repeated cycles of neon sputtering and annealing

 

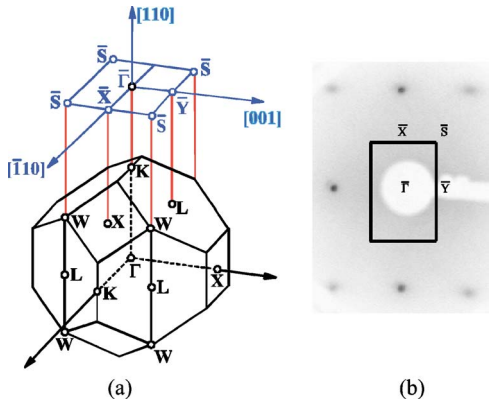


FIG. 1. (Color online) (a) Projection of the bulk Brillouin zone of the fcc Bravais lattice onto the (110) surface Brillouin zone. (b) LEED pattern of clean Al(110) and superimposed surface Brillouin zone.

at 400 °C until a $(1\times1)$ low-energy electron diffraction (LEED) pattern was obtained (Fig. 1). In the experiments at the synchrotron, contamination of the surface was additionally examined by means of x-ray photoemission spectroscopy (XPS).

The vacuum chamber located at the Technical University in Berlin was equipped with a helium discharge lamp as light source and a hemispherical VSW-HA50 electron energy analyzer with a total energy resolution of 90 meV. Two different beamlines were used for the experiments at the synchrotron. The vacuum chamber at one beamline[14] was equipped with a hemispherical 75-mm electron energy analyzer having a optimum total energy resolution of better than 15 meV. The actual resolution in the experiment determined by settings of the monochromator and the pass energy was around 100 meV. The spherical grating monochromator was optimized to cover the photon energy range from 8 to 150 eV. The other beamline[14] was equipped with a hemispherical electron energy analyzer of mean radius 50 mm (VGBlades). The resolution in this experiment was comparatively poor and limited to 200 meV. However, only the measurement of the dispersion of surface resonance $A$ was carried out with this setup. In all three setups the angle of incidence of the photon beam, $\theta_i$, was set to 45°. The electron energy analyzers were mounted on two-axis goniometers whose polar and azimuthal angles were adjusted to select electrons photoemitted at a sequence of points along a symmetry direction of the surface Brillouin zone (Fig. 1). At $\bar{\Gamma}$, $\bar{X}$, and $\bar{Y}$, the sample was aligned azimuthally such that the dispersion could be measured by changing only the polar angle. The ARUPS spectra were measured at room temperature.

## III. METHOD OF CALCULATION

The electronic structure of the (110) surface of aluminum has been calculated, within the framework of DFT, by the full-potential linearized-augmented plane-wave (FP-LAPW) method using the WIEN2K code.[15] In our calculation, the electron density is iterated to self-consistency in the field of atoms whose positions are determined from experiment. By examining the distribution of charge density in successive atomic layers of a supercell, we found that the enhanced charge density associated with features of the surface electronic structure of Al(110) extends over several (typically five) atomic layers. This is in contrast to transition metals, where the enhanced charge density associated with features of the surface electronic structure tends to be localized within one or two atomic layers. A preliminary calculation using a (110)-based supercell containing 6 unit cells of fcc Al (13 layers) and an atom-free region of equal thickness to represent the vacuum, as used in previous papers[12,13] to calculate bulk optical transitions on Al(110), failed to reproduce accurately the surface electronic structure. The metal-vacuum interface was represented by a (110)-based supercell containing 12 unit cells of fcc Al (25 layers), together with an atom-free region of equal thickness to represent the vacuum. The electronic structure of bulk Al projected onto the surface Brillouin zone was determined by calculating the electronic structure of a (110)-based supercell containing 24 unit cells of fcc Al (49 layers) with no vacuum region.

The energies and wave functions of the electron states were determined self-consistently by solving the Kohn-Sham equations of DFT. The calculation was carried out in the semirelativistic approximation, but the spin-orbit interaction was not included because it is expected to be negligible for the valence electrons in view of the low atomic number of aluminum ($Z=13$). Exchange and correlation were represented by a one-electron potential derived by Perdew *et al.*[16] in the GGA, an extension of the LDA that includes additional terms involving the gradient of the electron density that are particularly important at the surface. This GGA potential is regarded as being among the most accurate of the current generation of *ab initio* exchange-correlation potentials.

The conventional cubic lattice parameter of bulk Al at room temperature was taken to be $a_0=7.6526$ a.u.[11] The multilayer surface relaxation was represented by a contraction by 8.5% between the top layer and second layer, an expansion by 4.8% between the second layer and third layer, and a contraction by 3.9% between the third layer and fourth layer, all relative to the bulk interlayer spacing, as deduced from the room-temperature measurements of Busch and Gustafsson.[10] Each atom was represented by a spherical potential of radius $R_{MT}=2.5$ a.u., which is slightly smaller than one-half of the nearest-neighbor distance. It is essential to include nonspherical components of the potential because the surface electronic structure is very sensitive to the potential gradient at the metal-vacuum interface. The warping of the wave functions within each atomic sphere was represented by a spherical harmonic expansion that includes all terms up to $L=10$, and the warping of the interstitial potential was represented by a Fourier series expansion involving 34 430 plane waves.

In an ARUPS experiment, the binding energies $E$ of features of the surface electronic structure are measured relative to the Fermi energy $E_F$. To facilitate comparison between the calculated surface electronic structure and the experimental data, the Fermi energy must be determined with high accuracy. In the present calculation, the Brillouin zone integral for the Fermi energy was evaluated numerically on a grid of 1120 **k** vectors in the irreducible Brillouin zone, assuming a clean, ideally ordered, relaxed surface.

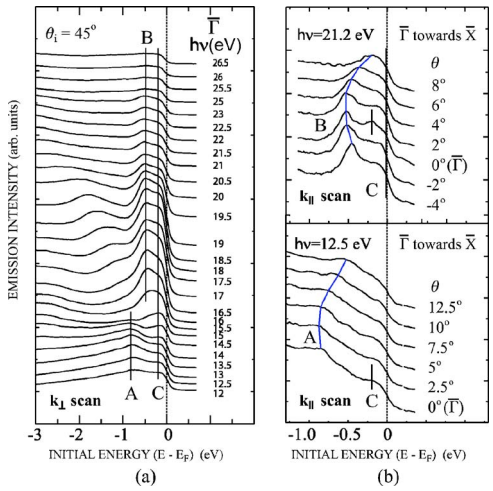


FIG. 2. (Color online) (a) Valence-band spectra at $\bar{\Gamma}$ for photon energies in the range 12.0–26.5 eV. Features *A* and *B*, which do not shift with the photon energy, correspond to surface resonances. The origin of the weak feature *C* was not determined. *A* is dominant for photon energies from 12.0–14.5 eV, while only *B* is seen from 16.5 to 23.0 eV. (b) Dispersion data from $\bar{\Gamma}$ towards $\bar{X}$ for *A* (lower panel) and *B* (upper panel). $\theta$ is the angle between the direction of emission and the surface normal.

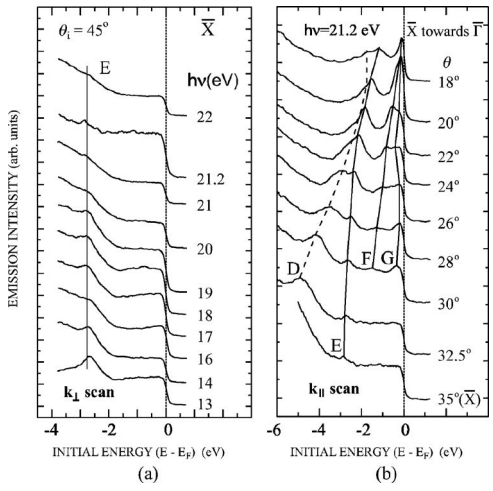


FIG. 3. (a) Valence-band spectra at $\bar{X}$ for photon energies in the range 13.0–22.0 eV. *E* has a binding energy of 2.7 eV and corresponds to a surface state. The origins of the other features, labeled *D*, *F*, and *G*, are discussed in the text. (b) Dispersion data for *E* from $\bar{X}$ towards $\bar{\Gamma}$. $\theta$ is the angle between the direction of emission and the surface normal.

## IV. RESULTS AND DISCUSSION

At any point of the surface Brillouin zone, surface states and surface resonances are discrete in energy while bulk states form a quasicontinuum. This makes it possible to distinguish experimentally between features of the surface and bulk electronic structures. The valence-band spectra are measured at high-symmetry points of the surface Brillouin zone over a range of photon energies, and those features whose binding energies are found to depend on the photon energy are attributed to the bulk electronic structure.[1] Surface states (states localized at the surface) can exist only in the pockets, which are projections onto the surface Brillouin zone of those regions of the bulk Brillouin zone where the density of bulk states vanishes. Elsewhere, surface states hybridize with delocalized states of the same symmetry to yield surface resonances (delocalized states that exhibit enhanced charge density at the surface). In the present work, features of the surface electronic structure that lie in the pockets are classified as surface states. Because our calculations show that the enhanced charge density associated with features of the surface electronic structure of Al(110) extends over several (typically the first five) atomic layers, other states are classified as surface resonances if their average charge densities are enhanced by at least 30% in the five outermost layers of the supercell and as bulk states otherwise.

At the synchrotron, photoemission spectra at a sequence of photon energies were measured at the symmetry points $\bar{\Gamma}$, $\bar{X}$, $\bar{Y}$, and $\bar{S}$ of the surface Brillouin zone. Figure 2–5 show stack plots of each set of data. We identified surface states or surface resonances at all of the symmetry points except $\bar{Y}$ (Fig. 4). In Table I, the measured and calculated binding energies of features of the surface electronic structure at high-symmetry points of the surface Brillouin zone are summarized and compared with the results of previous work. The dispersion of each feature was measured along the symmetry axes of the surface Brillouin zone. In Fig. 6, the measured

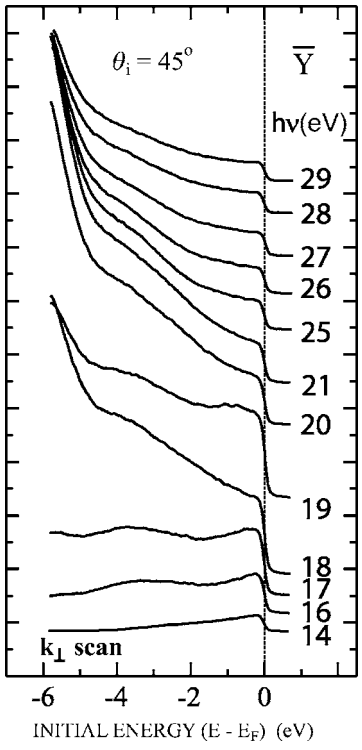


FIG. 4. Valence-band spectra at $\bar{Y}$ (for a binding energy of $E_b$ =4.5 eV) for photon energies in the range 14.0–29.0 eV. No features of the surface electronic structure were identified in the vicinity of $\bar{Y}$. $\theta$ is the angle between the direction of emission and the surface normal.

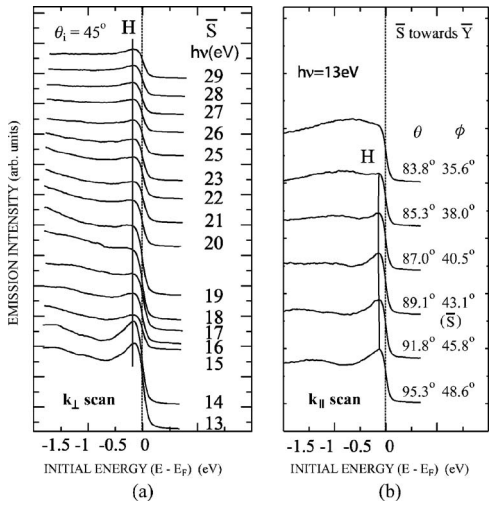


FIG. 5. (a) Valence-band spectra at $\bar{S}$ for photon energies in the range 13.0–29.0 eV. *H* has a binding energy of 0.2 eV and corresponds to a surface state. (b) Dispersion data for *H* from $\bar{S}$ towards $\bar{Y}$. $\theta$ and $\phi$ are the actual goniometer settings. At normal emission $\theta$=44.5° and $\phi$=0°.

dispersions deduced from our ARUPS data are compared with the results of our DFT-GGA calculation of the surface electronic structure in which surface relaxation is taken into account. The bulk energy bands calculated from a 48-layer supercell are superimposed. Features of the surface electronic structure in the vicinity of each high-symmetry point are discussed separately in the following sections.

### A. Surface electronic structure near $\bar{\Gamma}$

Our experimental photoemission spectra at $\bar{\Gamma}$, measured at photon energies in the range 12.0–26.5 eV, are shown in Fig. 2. Two strong features were identified: *A* (with a binding energy of 0.9 eV) and *B* (with a binding energy of 0.5 eV). These features do not shift with the photon energy, so they are attributed to the surface electronic structure. Because neither feature lies in a pocket, they are attributed to surface resonances. The cross sections for photoexcitation from *A* and *B* depend strongly on the photon energy. *A* dominates the ARUPS spectra below about 15.0 eV, and *B* dominates at higher energies. The dispersions of *A* and *B* from $\bar{\Gamma}$ towards $\bar{X}$ (i.e., along $\Sigma$) were measured with photons of energy 12.5 eV [Fig. 2(b), lower panel] and 21.2 eV [Fig. 2(b), upper panel], respectively. Both *A* and *B* disperse to higher energy from $\bar{\Gamma}$ towards $\bar{X}$ and are detected over an energy range of about 0.4 eV. In addition, a weak feature *C* appears in the spectra over the whole energy range. However, it was not possible to measure the dispersion of *C* because it is too close to the Fermi energy.

In Fig. 6, the results of our DFT-GGA calculation for the relaxed Al(110) surface are compared with the measured dispersions of *A* and *B*. The calculated electronic structure at $\bar{\Gamma}$ shows two *s*-like surface resonances, with binding energies 1.07 eV and 0.36 eV, which disperse to higher energy from $\bar{\Gamma}$ towards $\bar{X}$ and are observed over an energy range of about 0.4 eV. The binding energy of *A* corresponds to a surface resonance previously reported by Hansson and Flodstrom,[5] while to our knowledge *B* has not previously been reported. Hansson and Flodstrom were restricted to photon energies below 11.6 eV by the spectral range of their light source (a hydrogen discharge lamp), so the very small photoexcitation cross section of *B* over their energy range may explain why they did not detect this feature. Heinrichsmeier *et al.*[9] found only one feature of the surface electronic structure at $\bar{\Gamma}$, whose binding energy is consistent with *A*. Feature *C* was observed but not identified from the calculations.

### B. Surface electronic structure near $\bar{X}$

Our experimental photoemission spectra in the vicinity of $\bar{X}$ are shown in Fig. 3(a). At $\bar{X}$ we find a structure *E*, with binding energy 2.7 eV, which lies in a pocket and which does not shift for photon energies in the range from 13 eV to 22 eV. *E* is therefore attributed to a surface state. *E* disperses to higher energy from $\bar{X}$ towards $\bar{\Gamma}$ (i.e., along $\Sigma$) and is seen over an energy range of about 2.0 eV. Figure 6 shows that our DFT-GGA calculation for the relaxed Al(110) surface yields a closely spaced pair of surface states of $p_{001}$

TABLE I. Binding energies (in eV) and characters of features of the surface electronic structure of Al(110) at symmetry points (SS, surface state; SR, surface resonance).

| | Experimental | | Calculated | |
|---|---|---|---|---|
| Sym. point | Present work | Literature | Present work | Literature |
| $\bar{\Gamma}$ | 0.9 eV (SR) | 0.9 eV[a] (SR) | 1.07 eV (SR) | |
| $\bar{\Gamma}$ | 0.5 eV (SR) | | 0.36 eV (SR) | 0.45 eV[a] (SR) |
| $\bar{X}$ | | | 1.24 eV (SR) | 1.2 eV[b] (SR) |
| $\bar{X}$ | 2.7 eV (SS) | | 2.72 eV, 2.89 eV (SS) | 2.7 eV[a] (SS) |
| $\bar{S}$ | 0.2 eV (SS) | | 0.23 eV, 0.28 eV (SS) | 0.11 eV[a] (SS) |
| $\bar{S}$ | | | 1.09 eV (SR) | |

[a]Reference 9.
[b]Reference 8.

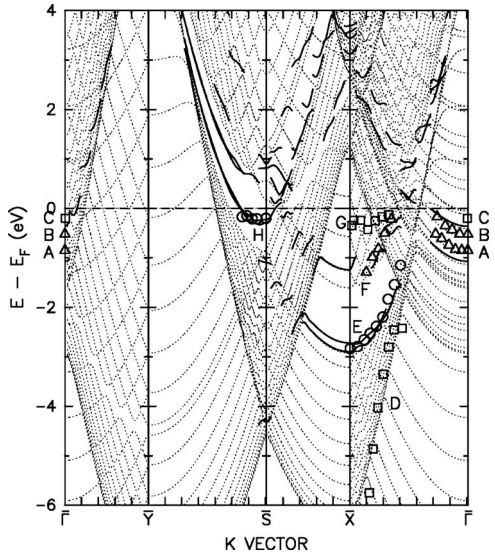


FIG. 6. (Color online) Binding energies and dispersions of features of the electronic structure of Al(110) as deduced from our ARUPS data. Surface states are plotted as circles, surface resonances are plotted as triangles, and other features are plotted as squares. The solid lines represent the surface band structure deduced from our DFT-GGA calculation for relaxed Al(110), and the bulk bands of Al(110) calculated from a 48-layer supercell are shown by dotted lines. As the number of layers is increased, the discrete bulk bands will fill in to yield regions of quasicontinuous bands separated by pockets.

symmetry, with binding energies 2.72 eV and 2.89 eV at $\bar{X}$, which are in excellent agreement with the experimentally observed binding energy and dispersion of $E$.

Three additional structures $D$, $F$, and $G$ appear in the experimental valence-band spectra taken close to $\bar{X}$ along $\Sigma$. Their dispersions are plotted in Fig. 6. Because none of these features is observed at $\bar{X}$, they are not seen in the $\boldsymbol{k}_\perp$ scans. Therefore, we have no experimental evidence as to whether they correspond to features of the surface or the bulk electronic structure.

In the energy regime of the present experiments, only direct ($\boldsymbol{k}$-conserving) interband optical transitions contribute to the structures observed in ARUPS. If at some energy the density of occupied bulk states in a highly localized region of the Brillouin zone is large, there will be many such transitions in a narrow range of photon energy, so in scans over $\boldsymbol{k}_\parallel$ and $\boldsymbol{k}_\perp$ a direct transition peak is likely to appear at that initial energy. The dispersion of $D$ follows closely a line in the projected band structure where, according to our FP-LAPW calculation, hybridization of a pair of overlapping nearly-free-electron-like bulk bands results in a large density of states that is highly localized in the bulk Brillouin zone. This suggests that $D$ may be due to direct optical transitions from bulklike electron states. $F$ follows a line of electron states that according to our calculation are bulk like but with charge densities that are somewhat enhanced at the surface (i.e., weak surface resonances). While $F$ is not seen in the ARUPS data at $\bar{X}$, our calculation predicts a surface resonance of $p_{110}$ symmetry with binding energy 1.24 eV at $\bar{X}$, which roughly matches the binding energy and dispersion of $F$. The experimental data and the results of our calculation are consistent in indicating that $G$ is not a feature of the surface electronic structure. While we did not determine the origin of $G$, it is probably due to bulk electronic states.

That $D$ was not predicted by previous calculations of the surface electronic structure[10,12] provides additional support to our interpretation in terms of direct optical transitions from bulklike initial states. The binding energy of $E$ is very similar to that of a surface state that was found by Hansson and Flodstrom close to $\bar{X}$ along $\Sigma$. Both the tight-binding calculation of Wang and Weber[8] and our DFT-GGA calculation predict a surface resonance at $\bar{X}$ that roughly matches the observed dispersion of $F$. This surface resonance was not predicted by the DFT-LDA calculation of Heinrichsmeier *et al.*

### C. Surface electronic structure near $\bar{Y}$

Our experimental photoemission spectra in the vicinity of $\bar{Y}$, shown in Fig. 4, yield no evidence for features that can be attributed to the surface electronic structure. The surface state at $\bar{Y}$ predicted by Heinrichsmeier *et al.*[9] is not reproduced by our calculation and is not supported by our experimental data.

### D. Surface electronic structure near $\bar{S}$

Our experimental photoemission spectra in the vicinity of $\bar{S}$ are shown in Fig. 5. $H$, with a binding energy of 0.2 eV, is observed for photon energies from 13 eV to 29 eV [Fig. 5(a)]. $H$ lies in a pocket and therefore corresponds to a surface state. The spectra measured at photon energy 13 eV [Fig. 5(b)] show that $H$ disperses little from $\bar{S}$ towards $\bar{Y}$. This is consistent with the result of our DFT-GGA calculation, which yields a closely spaced pair of surface states of $p_{110}$ symmetry, with binding energies 0.23 eV and 0.28 eV at $\bar{S}$, that disperse to higher energy both towards $\bar{X}$ and towards $\bar{Y}$. It is seen from Fig. 6 that our results for the binding energy and dispersion of $H$ are in very good agreement both with the results of the DFT-LDA calculation by Heinrichsmeier *et al.* and with the experimental data. Our calculation predicts an additional surface resonance at $\bar{S}$, with $p_{001}$ symmetry and binding energy 1.09 eV, that has not been detected experimentally. It might perhaps be expected that interband transitions from the surface state just below the Fermi level at $\bar{S}$ would contribute to the RAS for photon energies below about 1.0 eV. However, in metallic systems the reflectance anisotropy in this energy range is known to be dominated by Drude transitions, and interband transitions play only a minor role.

### E. Effects of surface relaxation

In the discussion above, our ARUPS data are compared with the results of DFT-GGA calculations in which the experimentally observed surface relaxation of Al(110) is taken

into account. We applied the same method of calculation to an ideally terminated (i.e., nonrelaxed) lattice in which the spacing between successive layers is equal to that of the bulk lattice. The calculated surface electronic structure of the ideally terminated lattice differs little from that shown in Fig. 6. Taking into account surface relaxation decreases the binding energy of surface resonance *A* by about 0.1 eV and increases the binding energies of surface states *E* and *H* by about 0.1 eV relative to the ideally terminated lattice, while on the scale of Fig. 6 the binding energy of surface resonance *B* is not significantly affected. In the present calculation, the surface relaxation is taken from the room temperature data of Busch and Gustafsson,[10] which show a contraction by 8.5% in the top layer, an expansion by 4.8% in the second layer, and a contraction by 3.9% in the third layer. Surface relaxation has no significant effect on the spacing of the deeper layers. As the binding energies and dispersions of features of the calculated surface electronic structure do not depend greatly on whether or not surface relaxation is taken into account, a calculation based on the LEED data of Mikkelsen *et al.*[11] is unlikely to yield a significantly different surface electronic structure.

Our calculations show that the charge density enhancement associated with features of the surface electronic structure of Al(110) extends over several (typically five) atomic layers. In the deformation potential approximation, the effect of surface relaxation on the binding energy of a feature of the surface electronic structure of Al(110) depends on the average dilation (the fractional change in atomic density) over this region. The average dilation in the first five layers is, from the experimental surface relaxation data quoted above,[10] approximately $(-8.5+4.8-3.9+0+0)/5=-1.5\%$. The small average dilation near the surface may account for the fact that the binding energies of the features of the calculated surface electronic structure depend only weakly on surface relaxation.

## V. CONCLUSIONS

The surface electronic structure of clean Al(110) in the vicinity of the high-symmetry points $\bar{\Gamma}$, $\bar{X}$, $\bar{Y}$, and $\bar{S}$ of the surface Brillouin zone has been investigated experimentally by ARUPS, and the results have been interpreted theoretically on the basis of DFT in the GGA. Structures *A*, *B*, *E*, and *H* in the ARUPS data are shown to correspond to surface states $(E,H)$ or surface resonances $(A,B)$, but we have no experimental evidence as to whether structures *C*, *D*, *F*, and *G* correspond to features of the surface or the bulk electronic structure. The dispersions of *A* and *B* were measured from $\bar{\Gamma}$ towards $\bar{X}$ (i.e., along $\Sigma$), those of *D*, *E*, *F*, and *G* from $\bar{X}$ towards $\bar{\Gamma}$ (also along $\Sigma$), and those of *H* from $\bar{S}$ towards $\bar{Y}$. To our knowledge, no previous measurements of the dispersions of features of the surface electronic structure of Al(110) have been reported. The calculated binding energies and the dispersions of the surface resonances *A* and *B* at $\bar{\Gamma}$, the surface state *E* at $\bar{X}$, and the surface state *H* at $\bar{S}$ are all in good agreement with the experimental data.

The surface resonance *A* and surface state *E* are consistent with features in the experimental data of Hansson and Flodstrom.[5] We also identified a surface resonance *B* at $\bar{\Gamma}$ and a surface state *H* at $\bar{S}$ that to our knowledge had not previously been observed. The results of our DFT-GGA calculation are in generally good agreement with those of the DFT-LDA calculation by Heinrichsmeier *et al.*[9] However, the surface state at $\bar{Y}$ predicted by Heinrichsmeier *et al.* is neither reproduced by our calculation nor supported by our experiment. Moreover, while both the tight-binding calculation of Wang and Weber[8] and the present calculation predict a surface resonance at $\bar{X}$ that roughly matches the measured dispersion of *F*, the calculation of Heinrichsmeier *et al.* does not yield this feature.

Taking into account surface relaxation slightly improves the overall agreement between the binding energies of features of the calculated surface electronic structure of Al(110) and the experimental data. It is suggested that the weak dependence of the binding energies of features of the surface electronic structure on surface relaxation is due to the small average dilation in the first few layers of the surface.

## ACKNOWLEDGMENTS

We thank Ch. Schultz for technical support at the Synchrotron in Aarhus, K. Stahrenberg for useful discussions, and Z. A. Ibrahim for helpful comments on the manuscript. This work was supported by the DFG under Contract No. Ri208/32, and by a Discovery Grant from the Natural Sciences and Engineering Research Council of Canada.

*Corresponding author. Email address: lee@physics.utoronto.ca

[1] S. Huefner, *Photoelectron Spectroscopy* (Springer-Verlag, Berlin, 1996).
[2] P. O. Gartland and B. J. Slagsvold, Solid State Commun. **25**, 489 (1978).
[3] J. K. Grepstad and B. J. Slagsvold, Phys. Scr. **25**, 813 (1982).
[4] K. H. Lee and K. J. Chang, Phys. Rev. B **49**, 2362 (1994).
[5] G. V. Hansson and S. A. Flodstrom, Phys. Rev. B **18**, 1562 (1978); Phys. Rev. B **19**, 3329(E) (1979).
[6] H. J. Levinson, F. Greuter, and E. W. Plummer, Phys. Rev. B **27**, 727 (1983).
[7] Ph. Hofmann, Ch. Søndergaard, S. Agergaard, S. V. Hoffmann, J. E. Gayone, G. Zampieri, S. Lizzit, and A. Baraldi, Phys. Rev. B **66**, 245422 (2002).
[8] X. W. Wang and W. Weber, Phys. Rev. B **35**, 7404 (1987).
[9] M. Heinrichsmeier, A. Fleszar, and A. G. Eguiluz, Surf. Sci. **285**, 129 (1993).
[10] B. W. Busch and T. Gustafsson, Surf. Sci. **415**, L1074 (1998).
[11] A. Mikkelsen, J. Jiruse, and D. L. Adams, Phys. Rev. B **60**, 7796 (1999).

[12] A. I. Shkrebtii and M. J. G. Lee, Prog. Surf. Sci. **74**, 283 (2003).
[13] Th. Herrmann, M. Gensch, M. J. G. Lee, A. I. Shkrebtii, N. Esser, W. Richter, and P. Hofmann, Phys. Rev. B **69**, 165406 (2004).
[14] S. V. Hoffmann, Ch. Søndergaard, Ch. Schultz, Z. Li, and Ph. Hofmann, Nucl. Instrum. Methods Phys. Res. A **523**, 441 (2004).
[15] P. Blaha, K. Schwarz, G. Madsen, D. Kvasnicka, and J. Luitz, computer code WIEN2K, An Augmented Plane Wave+Local Orbitals Program for Calculating Crystal Properties, Karlheinz Schwarz, Technical University of Wien, Austria, 2001.
[16] J. P. Perdew, J. A. Chevary, S. H. Vosko, K. A. Jackson, M. R. Pederson, D. J. Singh, and C. Fiolhais, Phys. Rev. B **46**, 6671 (1992).